

# First Step in the Reaction of Zerovalent Iron with Water

František Karlický\* and Michal Otyepka\*

Regional Centre of Advanced Technologies and Materials, Department of Physical Chemistry, Faculty of Science, Palacký University Olomouc, tr. 17 listopadu 12, 771 46 Olomouc, Czech Republic

**ABSTRACT:** Here we present a comprehensive quantum chemical study of the simplest model system for the reactions of nanoscale zerovalent iron, i.e., the gas-phase reaction of an iron atom with water, to identify a theoretical method that provides reasonably accurate geometries and thermochemical data for selected iron compounds along the reaction path (Fe, FeO, HFeOH, Fe(OH)<sub>2</sub>). The energies of selected stationary points on the ground electronic potential energy surface were systematically studied using HF and post-HF methods (MP2, MP3, MP4, CCSD, CCSD(T), CASSCF, MRCI) and selected DFT functionals (B3LYP, B97-1, BPW91, M06, M06-HF, M06-L, M06-2X and MPW1K) using various basis sets up to the complete basis set. Scalar relativistic effects were modeled using the Douglas–Kroll–Hess Hamiltonian up to the fourth order, and the effects of valence plus outer-core electronic correlation were also evaluated. The calculations showed that (i) dynamic electron correlation is crucial for accurate modeling of the reactions in question, (ii) the PES around the stationary points along the reaction path is rather flat, (iii) the single-point energies calculated at the CCSD(T)/CBS level are in reasonably good agreement with experimental measurements, (iv) it is difficult to interpret DFT energies in the absence of benchmarking against experimental data or results obtained at a level of theory that is known to accurately reproduce experimental results, (v) relativistic effects are relatively modest in this system but should be included if chemical accuracy is desired, and (vi) careful analysis of the multireference character of the system and potential spin contamination is important. The CCSD(T)-3s3p-DKH2/CBS method can be considered the gold standard for this reaction because calculations at this level are in good agreement with experimental atomic excitation energies and thermochemical data. The gas-phase activation energy of the reaction between Fe and H<sub>2</sub>O is 23.6 kcal/mol including the ZPVE correction ( $\Delta G_{298K}^{\ddagger} = 29.2$  kcal/mol), and HFeOH is a stable intermediate lying –31.2 kcal/mol below the reactants ( $\Delta G_{298K} = -25.4$  kcal/mol).

## I. INTRODUCTION

In recent years, reductive technologies for the decontamination of ground and wastewater using zerovalent iron (ZVI) and nanoscale zerovalent iron (nZVI) have become popular.<sup>1–4</sup> The high reductive capacity of ZVI has been known for some time.<sup>5–23</sup> A detailed understanding of the mechanisms by which reduction with nZVI proceeds will make it possible to optimize these processes and identify other potential uses of this material. In this respect, theoretical methods can provide relatively cheap and unique information on an atomic resolution.

However, the theoretical study of nZVI is complicated by the fact that is difficult to identify reasonable model systems. An nZVI particle with a radius of ~5 nm contains ~10<sup>4</sup>–10<sup>5</sup> iron atoms; such large systems are computationally intractable. As such, it is necessary to model the nZVI particle either as a cluster of a few iron atoms<sup>24,25</sup> or as a solid phase using Bloch's approach.<sup>26,27</sup> Unfortunately, both approaches have some drawbacks and limitations; in particular, the sizes of the systems involved and the need for periodic boundary conditions and simulation of electron correlation mean that it is necessary to use DFT methods, typically LDA or GGA functionals. This is a potentially serious issue because DFT functionals do not always provide systematic results for transition metal (TM) compounds, and the accuracy of their results is highly system dependent.<sup>28–30</sup> Moreover, even the best theoretical methods can generally only predict the thermochemistry of transition metal complexes with an accuracy of  $\pm 3$  kcal/mol,<sup>28,31,32</sup> whereas the goal of chemical accuracy (i.e., predictions that are within  $\pm 1$  kcal/mol of the experimental value) can be realized for main group compounds.

A better understanding of the reactivity of nZVI and iron in general would be useful because it could provide new insights into processes such as corrosion and steel production. However, there are numerous difficulties associated with computational studies of the reactivity of iron-containing compounds. First, the compounds may have several spin states; as such, it is necessary to identify the correct ground state<sup>33–36</sup> and to account for the possibility of crossing between states of different multiplicities along the reaction path.<sup>35</sup> Moreover, it is necessary to consider dynamic electron correlation to accurately model the behavior of iron compounds;<sup>37,38</sup> if a high degree of accuracy is required, scalar relativistic effects should also be considered<sup>28,39–41</sup> and it may be difficult to identify a suitable basis set.<sup>42</sup> Other complications may arise from the multireference character of certain iron-containing compounds. It is well known that unrestricted single-reference methods give rise to spin-contamination issues when applied to open-shell systems. In such cases, the unrestricted Hartree–Fock (uHF) wave function is not an eigenfunction of the total spin operator,  $S^2$ , and so the expectation value  $\langle S^2 \rangle$  may not be equal to  $S(S+1)$ ; as such, the obtained energies may be inaccurate. On the other hand, restricted open-shell Hartree–Fock (roHF) calculations with the right  $\langle S^2 \rangle$  are more computationally demanding, can generate unphysical results due to symmetry breaking artifacts, and do not allow correct spin polarization.<sup>43</sup> Therefore, it is sometimes necessary to use multi-reference methods for highly spin-contaminated systems,

Received: June 3, 2011

Published: July 18, 2011

especially for their transition states.<sup>38</sup> DFT methods are usually capable of predicting the properties of open-shell systems quite satisfactorily because they model correlation effects in a different way.<sup>43</sup> Finally, quantitative inconsistencies between DFT, CCSD(T), and CASPT2 results can be reconciled using quantum diffusion Monte Carlo theory.<sup>44</sup>

We present here a systematic quantum chemical study conducted to identify a method that provides reasonably accurate geometries and thermochemical data for selected iron compounds along the reaction coordinate for reaction of an iron atom with a water molecule ( $\text{Fe} + \text{H}_2\text{O}$ ). This reaction was chosen because it was expected that the data obtained would be useful in future studies of the reactions of nZVI with organic and inorganic pollutants. The chosen reaction represents the simplest model of nZVI reaction with water, but on the other hand, it allows one to benchmark considered quantum chemical methods against golden standards of quantum chemistry, e.g., CCSD(T)/CBS. The approach adopted in this work has previously been used to study the reaction of iron atoms with  $\text{CCl}_4$ <sup>45</sup> and cross validated with experimental data.<sup>46</sup> The considered reaction has previously been studied using both theoretical and experimental methods.<sup>47–51</sup>

The paper is organized as follows: the theoretical approaches and methods used are briefly described in section II. The results obtained are presented and discussed in section III. There are described systematic studies of the excitation energies of iron (section III.A) and the thermochemistry of  $\text{FeO}$  and  $\text{Fe}(\text{OH})_2$  (section III.B); the results obtained were compared to experimental data, in order to identify optimal methods and basis sets for modeling the reactions in question. Studies of the potential energy surfaces of the reaction between  $\text{Fe}$  and  $\text{H}_2\text{O}$  using various methods are discussed in section III.C, and the conclusions of the study are presented in section IV.

## II. METHODS

A set of calculations using selected ab initio methods was performed to identify important effects in the description of the model system. Dynamic electron correlation, which is important in molecular systems containing iron atoms,<sup>38</sup> was modeled using standard post-HF methods where possible. Both restricted and unrestricted open-shell variants were examined to avoid the problems mentioned in section I. Møller–Plesset perturbation theory, which is sometimes very sensitive to spin contamination,<sup>43</sup> was tested up to the fourth order. The coupled cluster methods (especially CCSD(T))<sup>28,39,52</sup> are quite efficient at reducing uHF spin contamination to acceptable levels,<sup>53</sup> so the results of uHF- and roHF-based coupled cluster calculations are often very similar. Because of the inherently multireference nature of many TM species, such single-reference computations can provide an inaccurate description of both static and dynamic electron correlation and it is necessary to check their legitimacy. Thus, not only spin contamination, but also  $T_1$  diagnostic,<sup>54,55</sup> which is a mathematically rigorous indication of the quality of an open-shell coupled cluster wave function, was monitored. A  $T_1$  diagnostic greater than 0.05 usually indicate some multireference character to the wave function.<sup>28,56</sup> For the simplest molecular system considered,  $\text{FeO}$ , higher correlation effects were investigated by comparison to results obtained using the complete active space SCF (CASSCF) and multireference CI (MRCI) methods. In the multireference calculations, the  $1\sigma$ – $6\sigma$  and  $1\pi$ – $2\pi$  orbitals were doubly occupied and kept in the inactive space as was the  $7\sigma$  orbital because of its almost pure oxygen  $2s$  character. The remaining 12

valence electrons were distributed between the 9 (MRCI(12,9)) valence orbitals ( $8\sigma$ – $10\sigma$ ,  $3\pi$ – $4\pi$ ,  $\delta$ ) corresponding to the iron 3d and 4s orbitals and the oxygen 2p orbital or between a set of 12 valence orbitals (MRCI(12,12), CASSCF(12,12)) consisting of the previous nine with additional  $11\sigma$  and  $5\pi$  orbitals. This resulted in 270 and 49 285 configurations, respectively. Scalar relativistic effects were studied using the Douglas–Kroll–Hess (DKH) Hamiltonian; calculations of the zeroth (DKH0), second (DKH2), and fourth order (DKH4) were performed.

We also sought to identify a less computationally demanding quantum chemical method that could accurately describe the model system for use in future studies and therefore examined the performance of various DFT methods. A limited set of functionals was considered; those selected have often been used for studying TM compounds or recommended as being particularly useful for studying the thermochemistry of TM complexes and the transition structures encountered in their reactions. The hybrid B3LYP functional<sup>57</sup> has been used in many studies of this kind, having been used to study the reaction between  $\text{Fe}$  and  $\text{H}_2\text{O}$  by Plane et al.,<sup>47,51</sup> Mebel and Hwang,<sup>48</sup> and Zhang et al.<sup>49</sup> Gutsev et al. used the BPW91 exchange-correlation functional<sup>58,59</sup> to study the interactions of small iron clusters with individual molecules of water<sup>50</sup> and nitrogen monoxide<sup>60</sup> and with a carbon atom;<sup>61</sup> these authors also used this functional to study  $\text{FeO}_n$  and  $\text{FeO}_n^-$  clusters.<sup>62</sup> The B97-1 functional has been used to model the interactions of molecules with water and in small water clusters.<sup>63,64</sup> Recently, Zhao and Truhlar developed a new set of functionals called the M06 suite for the study of the thermochemistry, thermochemical kinetics, noncovalent interactions, and excited states of main group and transition metal compounds.<sup>65</sup> We examined the performances of the hybrid meta exchange-correlation M06 and M06-2X functionals, the full Hartree–Fock M06-HF functional, and the M06-L local functional.<sup>66</sup> The older hybrid-GGA MPW1K functional,<sup>67</sup> which was designed for accurate computation of reaction barriers, was also considered.

Previous studies in this area<sup>47–49,51</sup> used Pople's basis sets, i.e., 6-31G\*\*, 6-311G\*\*, 6-311+G(3df,2p). These sets were also used in this work, but we performed a major part of our calculations using the correlation-consistent basis sets (cc-pVnZ, aug-cc-pVnZ,  $n = \text{D, T, Q}$ ), which were recently extended to cover the 3d elements by Balabanov and Peterson.<sup>52</sup> The basis sets recommended by Balabanov and Peterson for iron (cc-pVnZ-DK, aug-cc-pVnZ-DK; cc-pwCVnZ-DK)<sup>52</sup> were employed in scalar relativistic calculations and calculations of valence plus outer-core (3s3p3d4s) electron correlation; these sets were obtained from the basis set exchange database.<sup>68</sup> Correlation-consistent basis sets can be used to extrapolate to the complete basis set (CBS) limit. Although the DFT methods are much less basis set dependent and this convergence is not necessarily guaranteed for DFT, it has been shown (see, e.g., ref 31 or 32 and references therein) that for some molecules quadruple- $\zeta$  or higher basis sets are required for saturation in DFT, and CBS extrapolation has been used successfully. Two CBS extrapolation schemes were utilized here. In the first (CBS1), the HF and correlation energies are extrapolated separately, as is usually done when studying main group species. The HF energy was extrapolated using the two-point scheme described by Halkier et al.<sup>69</sup>

$$E_{\infty}^{\text{HF}} = E_n^{\text{HF}} - \frac{E_n^{\text{HF}} - E_{n+1}^{\text{HF}}}{1 - \exp(-B)} \quad (1)$$

This scheme has also been recommended for use with TMs, albeit with a different value for parameter  $B$ .<sup>70</sup> The correlation

**Table 1.** Calculated Excitation Energies of Iron (kcal/mol) for the  $^5\text{D} \rightarrow ^5\text{F}$  (a),  $^5\text{D} \rightarrow ^3\text{F}$  (b), and  $^5\text{D} \rightarrow ^7\text{D}$  (c) Transitions<sup>a</sup>

| method  | uCCSD(T)                            | uCCSD(T)-DKH2                       | uCCSD(T)-3s3p-DKH2                  |
|---|-------------------------------------|-------------------------------------|-------------------------------------|
| basis set   | cc-pVnZ                             | cc-pVnZ-DK                          | cc-pwCVnZ-DK                        |
| (a) $^5\text{D} (4s^23d^6) \rightarrow ^5\text{F} (4s^13d^7)$     |                                     |                                     |                                     |
| $n = \text{T}$  | 22.6                                | 28.5                                | 25.9                                |
| $n = \text{Q}$  | 20.2                                | 26.1                                | 23.0                                |
| CBS1  | 18.5                                | 24.4                                | 21.0                                |
| CBS2  | 18.4                                | 24.3                                | 20.9                                |
| exp. <sup>b</sup>   |                                     |                                     | 20.1                                |
| (b) $^5\text{D} (4s^23d^6) \rightarrow ^3\text{F} (4s^13d^7)$     |                                     |                                     |                                     |
| $n = \text{T}$  | 31.5                                | 37.8                                | 36.4                                |
| $n = \text{Q}$  | 29.0                                | 35.4                                | 33.4                                |
| CBS1  | 27.3                                | 33.7                                | 31.3                                |
| CBS2  | 27.2                                | 33.6                                | 31.2                                |
| exp. <sup>b</sup>   |                                     |                                     | 34.0                                |
| (c) $^5\text{D} (4s^23d^6) \rightarrow ^7\text{D} (4s^13d^64p^1)$ |                                     |                                     |                                     |
| $n = \text{T}$  | 52.5                                | 54.4                                | 56.0                                |
| $n = \text{Q}$  | 53.5                                | 55.4                                | 57.0                                |
| CBS1  | 54.3                                | 56.2                                | 57.7                                |
| CBS2  | 54.3                                | 56.2                                | 57.7                                |
| exp. <sup>b</sup>   |                                     |                                     | 54.7                                |
|   |                                     |                                     |                                     |
|   | $^5\text{D} \rightarrow ^5\text{F}$ | $^5\text{D} \rightarrow ^3\text{F}$ | $^5\text{D} \rightarrow ^7\text{D}$ |
| (d) uCCSD(T) calculations for smaller basis sets                  |                                     |                                     |                                     |
| 6-31G**   | 73.6                                | 79.6                                | 58.3                                |
| 6-311G**  | 41.4                                | 48.5                                | 135.7                               |
| 6-311G(3df,2p)  | 20.7                                | 29.6                                | 53.5                                |
| cc-pVDZ   | 29.3                                | 37.6                                | 49.5                                |

<sup>a</sup> Results for other basis sets tested in this work are also shown (d).<sup>b</sup> Reference 76; the spin-orbit effect has been removed using the experimental fine-structure splitting.

energy was extrapolated from two points using the following expression<sup>71</sup>

$$E_{\infty}^{\text{corr}} = \frac{n^3 E_n^{\text{corr}} - m^3 E_m^{\text{corr}}}{n^3 - m^3} \quad (2)$$

$E_{\infty}$  and  $E_n$  denote the extrapolated energy and energy for a basis set of  $n$ - $\zeta$  cardinality, respectively. Equation 2 was also used in the second extrapolation scheme (CBS2) using the total energies only as in ref 52. CBS extrapolations were performed from bases of triple- $\zeta$  and quadruple- $\zeta$  cardinality (i.e.,  $n = 3$ ,  $m = 4$ ).

Most of the calculations reported in this work were performed using the Gaussian 09 package;<sup>72</sup> the Molpro 2006 package<sup>73</sup> was used for multireference calculations. The stability of the obtained wave functions was always checked. In cases of bad SCF convergence, which is often caused by a small HOMO–LUMO gap, we used the “level-shifting” method,<sup>74</sup> which shifts the virtual orbitals to a higher energy to increase the HOMO–LUMO gap, and/or techniques that fractionally occupy orbitals around the Fermi energy during the SCF cycles (Fermi broadening).<sup>75</sup> The quadratically convergent SCF algorithm (which can only be employed with unrestricted methods in Gaussian 09) was generally more effective at forcing SCF convergence than the direct inversion in

the iterative subspace (DIIS) algorithm. The nature of all identified stationary points on the PES was tested by examining the eigenvalues of the Hessian matrix, and the intrinsic reaction coordinate method was used to verify the correspondence of transition structures to their adjacent minima.

### III. RESULTS AND DISCUSSION

**III.A. Excitation Energies of Atomic Iron.** In order to assess the quality of the CCSD(T) method, which we intended to use as our benchmark, we computed selected excitation energies of the iron atom. The calculated energies for the  $^5\text{D} \rightarrow ^5\text{F}$ ,  $^5\text{D} \rightarrow ^3\text{F}$ , and  $^5\text{D} \rightarrow ^7\text{D}$  transitions are shown along with the experimental values<sup>76</sup> in Table 1. The high quality of the coupled cluster wave functions for the  $^5\text{D}$  and  $^5\text{F}$  states was demonstrated by their  $\langle S^2 \rangle$  and  $T_1$  diagnostic values, which were less than 6.02 and 0.03, respectively. For the CBS limit energies, inclusion of scalar relativity through the DKH2 Hamiltonian and cc-pVnZ-DK basis set worsened the agreement with experiment; the calculated relativistic effect was 5.9 kcal/mol. On the other hand, inclusion of 3s3p electron correlation (with the cc-pwCVnZ-DK basis set) reduced the calculated  $^5\text{D} \rightarrow ^5\text{F}$  excitation energy by 3.4 kcal/mol, giving very good agreement with the experimental value; the difference between the calculated and measured values in this case is only 0.8 kcal/mol. It is worth noting that our results (obtained with Gaussian09 using the uCCSD(T) method) are consistent with those of previous calculations<sup>39</sup> using the open-shell variant of CCSD(T) implemented in MOLPRO; the differences between the two sets of calculated results were 0.7 kcal/mol and less than 0.1 kcal/mol appear for calculations including valence correlation and 3s3p3d4s correlation, respectively.

The calculated excitation energies for the  $^5\text{D} \rightarrow ^3\text{F}$  and  $^5\text{D} \rightarrow ^7\text{D}$  transitions do not exhibit such good agreement with the experimental data as was the case for the  $^5\text{D} \rightarrow ^5\text{F}$  transition (see Table 1) but are still within the chemical accuracy for TM (3 kcal/mol). This may be due to high-spin contamination for the  $^3\text{F}$  state, for which  $\langle S^2 \rangle \approx 3$  (although the value of the  $T_1$  diagnostic in this case remained within acceptable limits,  $<0.03$ ); the  $^7\text{D}$  state wave function is not contaminated ( $\langle S^2 \rangle = 12.00$ ,  $T_1 = 0.01$ ). We also calculated the excitation energies using Pople's basis sets which have been used in previous studies (cf. Methods) and the cc-pVDZ basis set. The smaller basis sets (6-31G\*\*, 6-311G\*\*, and cc-pVDZ) perform significantly poor (Table 1d).

**III.B. Heats of Formation of FeO and Fe(OH)<sub>2</sub>.** We also compared the calculated thermochemical data to available experimental data for FeO and Fe(OH)<sub>2</sub>. Theoretical heats of formation  $\Delta H_f$  at  $T = 0$  K were calculated by subtracting the calculated atomization energies from the known heats of formation of isolated atoms. Atomic  $\Delta H_f$  values were taken from NIST-JANAF tables.<sup>77</sup> It should be noted that the experimental heat of formation for FeO in the gas phase is not well established at the present time, as can be seen from the last lines of Table 2. CCSD and the various DFT methods considered here give very different results (column 5 of Table 2) for the quintet ground state<sup>78,79</sup> of FeO ( $^5\Delta$ ; Fe( $4s^03d^64p^{0.2}$ ) O( $2s^{1.9}2p^{4.9}$ )). However, the CCSD(T)/CBS values for  $\Delta H_f$  calculated as single-point energies for the same geometries are surprisingly consistent and reasonably close to the experimental values.<sup>77,80,81</sup> This implies that the CCSD(T)  $\Delta H_f$  values are insensitive to the length of the Fe–O bond (cf. the second and last columns of Table 2: a difference of 0.021 Å in the Fe–O distance



**Table 2.** Bond Lengths [Å], Vibrational Frequencies [ $\text{cm}^{-1}$ ],  $\langle S^2 \rangle$ , and Heats of Formation  $\Delta H_f$  [kcal/mol] of FeO at 0 K, Calculated Using Unrestricted Methods and the cc-pVTZ Basis Set (the geometry of FeO was fully optimized)<sup>a</sup>

| method | $b(\text{Fe}-\text{O})$ | freq             | $\langle S^2 \rangle$ | $\Delta H_f^b$ | $\Delta H_f^c$              |
|--------|-------------------------|------------------|-----------------------|----------------|-----------------------------|
| CCSD   | 1.6184                  | 832              | 6.791                 | 86.9           | 67.6 (69.7, 68.1)           |
| B3LYP  | 1.6095                  | 911              | 6.038                 | 57.7           | 67.7                        |
| B97-1  | 1.6124                  | 903              | 6.030                 | 59.9           | 67.7                        |
| BPW91  | 1.6047                  | 922              | 6.018                 | 34.9           | 67.7                        |
| M06    | 1.6118                  | 926              | 6.037                 | 72.4           | 67.7                        |
| M06-L  | 1.6130                  | 915              | 6.130                 | 53.4           | 67.7                        |
| M06-2X | 1.6257                  | 955              | 6.523                 | 88.9           | 67.8                        |
| MPW1K  | 1.6125                  | 901              | 6.018                 | 82.2           | 67.7                        |
| exp.   | 1.616 <sup>d</sup>      | 880 <sup>e</sup> |                       |                | 60.0 $\pm$ 5.0 <sup>h</sup> |
|        | 1.57 <sup>f</sup>       | 965 <sup>f</sup> |                       |                | 61.9 $\pm$ 4.8 <sup>i</sup> |
|        |                         | 882 <sup>g</sup> |                       |                | 65.5 $\pm$ 3.0 <sup>j</sup> |
|        |                         |                  |                       |                | 64.8 $\pm$ 3.0 <sup>k</sup> |

<sup>a</sup> The rightmost column shows the heats of formation calculated using the uCCSD(T)/CBS2 method for the same geometries. Values obtained using the CCSD(T)-DKH2/CBS2 method using the cc-pVnZ-DK basis sets and additional 3s3p electron correlation are shown in parentheses in the rightmost column of the first row. <sup>b</sup> Values calculated using the methods indicated in the first column. <sup>c</sup> Values calculated using the CCSD(T)/CBS2 method for geometries obtained by optimization using the method indicated in the first column. <sup>d</sup> Reference 79. <sup>e</sup> Reference 78. <sup>f</sup> Reference 77. <sup>g</sup> Reference 84. <sup>h</sup> Reference 77; adopted from several values cited therein (47.2, 65.7  $\pm$  23.1, 60.1  $\pm$  11.6, 59.8  $\pm$  5, and 52.2 kcal/mol at 298.15 K). <sup>i</sup> Reference 80. <sup>j</sup> Reference 81. <sup>k</sup> Reference 47 (revised data from ref 81; see ref 47 Table S, footnote i).

corresponds to a 0.1 kcal/mol difference in the CCSD(T)/CBS energies). This finding suggests that the potential energy surface (PES) is flat in the vicinity of the minimum. In addition, we also checked the influence of the basis set on the geometry of the FeO molecule. Bond lengths optimized with methods of Table 2 were very similar when cc-pVTZ or aug-cc-pVQZ basis sets were used: differences were typically smaller than 0.003 Å. This shows that the cc-pVTZ basis set is adequate for geometry optimizations and that the error in bond length associated with the use of a finite basis of triple- $\zeta$  cardinality is much less than the uncertainty associated with the choice of DFT functional.

The potential energy curve around the minimum on the FeO potential energy curve (Figure 1) was calculated using various methods in order to compare the performance of single and multireference methods, to evaluate the differences between the restricted open-shell and unrestricted approaches, to assess the influence of scalar relativistic effects calculated on various levels, and to confirm the expected flatness around the minimum. For the uHF wave function an  $\langle S^2 \rangle$  value of  $\sim 6.7$  was obtained (compared to an expected  $S(S+1)$  of 6; cf. Table 2), and the CC  $T_1$  diagnostic was  $\sim 0.1$  (values above 0.05 indicate that the wave function may have multireference character<sup>28</sup>). On the other side, the MRCI(12,12) leading configuration for  $S = 2$  was (core)  $8\sigma^2 3\pi^4 9\sigma 1\delta^3 4\pi^2$ , with weight 82%, 78%, 75%, and 71% for bond length 1.5, 1.62, 1.7, and 1.8 Å, respectively; this corresponds to the  $^5\Delta$  state (in the  $C_{\infty v}$  group, i.e.,  $^5A_1$  or  $^5A_2$  for  $C_{2v}$ ) in agreement with a recent theoretical study.<sup>82</sup> The geometries corresponding to ro-methods are slightly more diffuse than geometries calculated by u-methods. However, this difference is energetically insignificant because the increase in

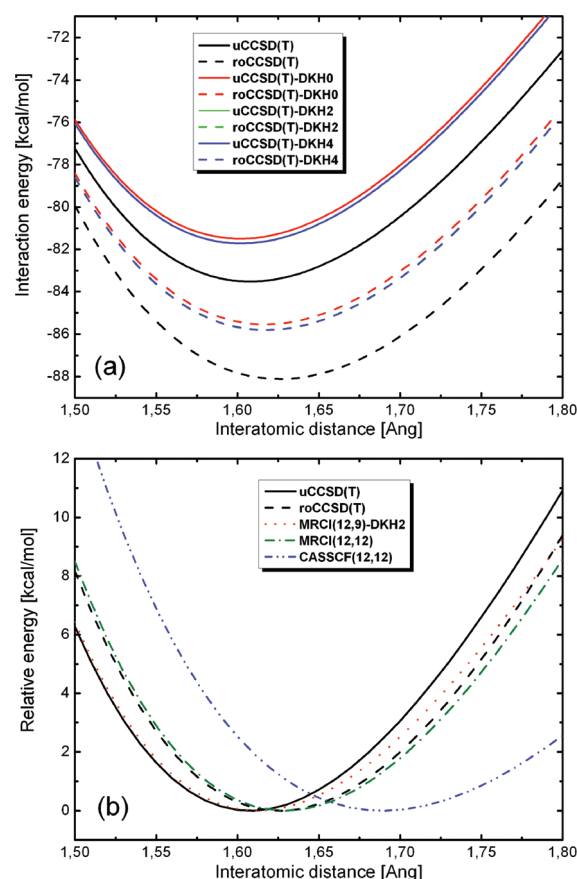


**Figure 1.** (a) Quintet FeO interaction potentials constructed from 30 points for unrestricted (solid lines) and restricted open-shell (dashed lines) CCSD(T) methods with the cc-pVTZ basis set using several Hamiltonians: nonrelativistic (black lines), scalar relativistic DKH0 (red lines), DKH2 (green lines; these are coincident with the blue lines), and DKH4 (blue lines). (b) Relative energies reported with respect to the minima of the individual curves obtained using multireference methods. The nonrelativistic unrestricted (black line) and restricted open (dashed black line) CCSD(T) data from a are included for comparative purposes; in addition, MRCI(12,12), MRCI(12,9)-DKH2, and CASSCF(12,12) curves are also shown (green dot-dashed, red dotted, and blue dash-dotted lines, respectively).

length of around 0.03 Å magnitude at the minima of the depicted curves is associated with energy differences of 0.5 kcal/mol or less (Figure 1a). The bond lengths obtained using the multireference CASSCF(12,12) method, which lacks dynamic electron correlation, are noticeably greater than those obtained in MRCI calculations (Figure 1b), which account for both static and dynamic electron correlation. This observation illustrates the point that inclusion of dynamic electron correlation is important for reliable geometry optimization. Inclusion of scalar relativistic effects did not alter the position of the energy minima (Figure 1a). We also note that using the DKH2 Hamiltonian introduced a systematic reduction in all of the calculated energies of around 2.1 kcal/mol, while introduction of additional 3s3p electron correlation made all of the calculated energies about 1.6 kcal/mol higher (see also Table 2).

We also carried out similar benchmark calculations for  $\text{Fe}(\text{OH})_2$ . The experimental heats of formation for  $\text{Fe}(\text{OH})_2$  in the gas phase seem to be more precisely determined than for FeO (see Table 3), although the accuracy of the reported experimental error of 0.5 kcal/mol has been questioned.<sup>83</sup> Table 3 reports the heats of

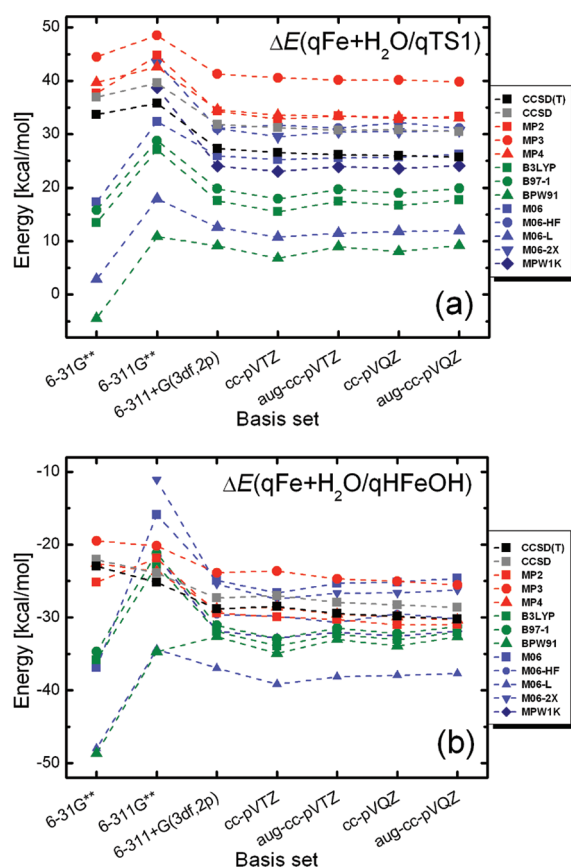
**Table 3.** Bond Lengths [Å], Dihedral Angles [deg],  $\langle S^2 \rangle$ , and Heats of Formation  $\Delta H_f$  [kcal/mol] of  $\text{Fe}(\text{OH})_2$  at 0 K<sup>a</sup>

| method | $b(\text{Fe}-\text{O})$ | $b(\text{O}-\text{H})$ | $d(\text{HOO}'\text{H}')$ | $\langle S^2 \rangle$ | $\Delta H_f^b$ | $\Delta H_f^c$           |
|--------|-------------------------|------------------------|---------------------------|-----------------------|----------------|--------------------------|
| CCSD   | 1.804                   | 0.953                  | 95.42                     | 6.017                 | −45.1          | −72.3 (−69.6)            |
| B3LYP  | 1.791                   | 0.957                  | 89.48                     | 6.010                 | −66.7          | −72.5                    |
| B97-1  | 1.792                   | 0.956                  | 88.90                     | 6.011                 | −65.4          | −72.5                    |
| BPW91  | 1.787                   | 0.967                  | −85.26                    | 6.008                 | −75.1          | −72.4                    |
| M06    | 1.780                   | 0.954                  | 86.76                     | 6.021                 | −59.5          | −72.1                    |
| M06-L  | 1.788                   | 0.955                  | 87.23                     | 6.016                 | −65.4          | −72.5                    |
| M06-2X | 1.809                   | 0.953                  | 98.92                     | 6.014                 | −63.7          | −72.3                    |
| MPW1K  | 1.788                   | 0.946                  | 95.90                     | 6.013                 | −50.0          | −73.6                    |
| exp.   | 1.8 <sup>d</sup>        | 0.96 <sup>d</sup>      |                           |                       |                | −77.2 ± 0.5 <sup>d</sup> |

<sup>a</sup> All calculations reported in this table were performed using unrestricted methods and the cc-pVTZ basis set except for those reported in the last column, which shows the uCCSD(T)/CBS2 values for the same geometries. Values obtained using the CCSD(T)-DKH2/CBS2 method using the cc-pVnZ-DK basis set are reported in parentheses in the first row (rightmost column). <sup>b</sup> Values calculated using the methods indicated in the first column. <sup>c</sup> Values calculated using the CCSD(T)/CBS2 method for geometries obtained by optimization at the level indicated in the first column. <sup>d</sup> Reference 77.

**Table 4.** Single-Point Energy Differences (in kcal/mol, calculated using unrestricted methods) for Three Quintet Configurations ( $\text{Fe} + \text{H}_2\text{O}$ , TS1, and  $\text{HFeOH}$ ) Optimized Using the B3LYP Functional

| method  | $\Delta E(\text{qFe}+\text{H}_2\text{O}/\text{qTS1})$ |         | $\Delta E(\text{qFe}+\text{H}_2\text{O}/\text{qHFeOH})$ |         |
|---------|---|---------|---|---------|
|         | cc-pVTZ   | cc-pVQZ | cc-pVTZ   | cc-pVQZ |
| CCSD(T) | 26.6  | 26.0    | −28.5   | −29.9   |
| CCSD    | 31.2  | 30.8    | −27.0   | −28.3   |
| MP2     | 32.8  | 32.9    | −29.9   | −31.0   |
| MP3     | 40.6  | 40.1    | −23.6   | −25.0   |
| MP4     | 33.6  | 33.2    | −28.6   | −29.9   |
| B3LYP   | 15.5  | 16.7    | −33.9   | −31.1   |
| B97-1   | 17.9  | 19.0    | −32.9   | −32.2   |
| BPW91   | 6.8   | 8.0     | −35.0   | −33.9   |
| M06     | 25.2  | 25.7    | −26.6   | −25.2   |
| M06-HF  | 31.7  | 32.2    | −29.8   | −29.5   |
| M06-L   | 10.7  | 11.8    | −39.2   | −38.0   |
| M06-2X  | 29.5  | 30.5    | −27.5   | −26.7   |
| MPW1K   | 23.0  | 23.6    | −32.8   | −32.5   |

**Figure 2.** Single-point energy differences (in kcal/mol, calculated using unrestricted methods) for three quintet configurations ( $\text{Fe} + \text{H}_2\text{O}$ , TS1, and  $\text{HFeOH}$ ) optimized using the B3LYP functional and their dependences on the chosen basis set: (a)  $\text{qFe}+\text{H}_2\text{O}/\text{qTS1}$ , (b)  $\text{qFe}+\text{H}_2\text{O}/\text{qHFeOH}$ .

formation of  $\text{Fe}(\text{OH})_2$  calculated using various methods. Overall, the trends in these data are similar to those observed in the case of

$\text{FeO}$ . Once again, the  $\Delta H_f$  values obtained with the different methods are somewhat inconsistent, but the energies obtained from single-point CCSD(T) calculations at the various optimized geometries are all very similar. We therefore believe that the region surrounding the global minimum on the PES of  $\text{Fe}(\text{OH})_2$  is very flat. Inclusion of the DKH2 Hamiltonian reduces all of the calculated energies by 2.3–2.9 kcal/mol.

In general, it is not so surprising that different DFT functionals will exhibited varied performance when predicting the thermochemical data of TM compounds. Recently, Yang et al.<sup>30</sup> studied 94 systems containing first-row TMs from Ti to Zn with 12 different functionals. The best mean unsigned error (MUE; the difference between the experimental and calculated values of  $\Delta H_f$ ) for systems containing iron atoms was 12.2 kcal/mol; the worst was 43.5 kcal/mol (see Table 4 of ref 30).

**III.C. Reaction of Fe with  $\text{H}_2\text{O}$ .** A systematic study of the energies of selected stationary points on the ground state electronic quintet PES of the  $\text{Fe} + \text{H}_2\text{O}$  system was conducted, and the energy differences between the stationary points were calculated to complete the benchmark thermochemical data discussed in sections IIIA and IIIB. We focused on the most important stationary points in the reaction mechanism, namely, those corresponding to the reactants ( $\text{qFe}+\text{H}_2\text{O}$ ), the global minimum ( $\text{qHFeOH}$ ), and the transition state between them ( $\text{qTS1}$ ). We carried out single-point unrestricted calculations on B3LYP-optimized geometries using various basis sets. Figure 2 shows how varying the basis set affects the energy differences encountered along the reaction pathway. The smaller basis sets used in some previous studies<sup>47–49,51</sup> (6-31G\*\* and 6-311G\*\*) do not provide reliable results for the studied reaction (cf. also ref 42). Table 4 compares the energy differences calculated using unrestricted methods with the cc-pVTZ and cc-pVQZ basis sets. All methods perform rather poorly (with respect to CCSD(T)) for the TS (MUE = 8.3 and 7.9 kcal/mol for the TZ and QZ basis sets, respectively) but are significantly better at the minima (MUE = 3.6 and 3.0). In the case of  $\text{FeO}$ , accurate results could be obtained without having to use augmented basis sets; to verify that this remained true, we computed CBS2 energies for basis sets

Table 5. Energy Differences (in kcal/mol) for Stationary Points on the Ground Quintet Surface of the Fe + H<sub>2</sub>O Reaction<sup>a</sup>

| method  | $\Delta E$ (without ZPE correction) |              |                   |                   | ZPE corr.    | $\Delta E$ (with ZPE correction) |              |                   |                   | $\Delta G_{\text{corr}}$ | $\Delta G$        |
|---|-------------------------------------|--------------|-------------------|-------------------|--------------|----------------------------------|--------------|-------------------|-------------------|--------------------------|-------------------|
|   | first column                        | CCSD(T)-DKH2 | CCSD(T)-3s3p-DKH2 | CCSD(T)-3s3p-DKH2 | first column | first column                     | CCSD(T)-DKH2 | CCSD(T)-3s3p-DKH2 | CCSD(T)-3s3p-DKH2 | first column             | CCSD(T)-3s3p-DKH2 |
|   | basis set on Fe                     | cc-pVTZ      | cc-pVnZ           | cc-pVnZ-DK        | cc-pwCVnZ-DK | cc-pVTZ                          | cc-pVTZ      | cc-pVnZ           | cc-pVnZ-DK        | cc-pwCVnZ-DK             | cc-pwCVnZ-DK      |
| $\Delta E(\text{qFe}+\text{H}_2\text{O}/\text{qFe}\cdots\text{OH}_2)$ |                                     |              |                   |                   |              |                                  |              |                   |                   |                          |                   |
| B3LYP   | −10.2                               | −3.7         | −2.7              | −2.9              | 1.0          | −9.1                             | −2.7         | −1.6              | −1.8              | 6.3                      | 3.4               |
| B971  | −8.7                                | −3.7         | −2.7              | −2.9              | 1.1          | −7.7                             | −2.7         | −1.6              | −1.8              | 6.3                      | 3.4               |
| BPW91   | −10.2                               | −3.5         | −2.5              | −2.7              | 0.9          | −9.3                             | −2.6         | −1.6              | −1.8              | 6.1                      | 3.4               |
| M06   | −7.7                                | −3.7         | −2.7              | −2.9              | 0.9          | −6.7                             | −2.7         | −1.8              | −2.0              | 6.1                      | 3.2               |
| M06-HF  | −6.1                                | −3.4         | −2.5              | −2.6              | 0.8          | −5.3                             | −2.6         | −1.7              | −1.8              | 5.7                      | 3.0               |
| M06-L   | −12.4                               | −3.7         | −2.7              | −2.9              | 0.8          | −11.6                            | −2.9         | −1.9              | −2.1              | 5.9                      | 3.0               |
| M06-2X  | −5.3                                | −3.7         | −2.8              | −2.9              | 0.9          | −4.4                             | −2.9         | −1.9              | −2.1              | 6.0                      | 3.0               |
| MPW1K   | −5.6                                | −3.8         | −2.8              | −2.9              | 1.2          | −4.3                             | −2.5         | −1.5              | −1.7              | 6.4                      | 3.4               |
| average   | −8.3                                | −3.6         | −2.7              | −2.8              | 1.0          | −7.3                             | −2.7         | −1.7              | −1.9              | 6.1                      | 3.2               |
| MUE   | 2.1                                 | 0.1          | 0.1               | 0.1               | 0.1          | 2.1                              | 0.1          | 0.1               | 0.1               | 0.2                      | 0.2               |
| $\Delta E(\text{qFe}+\text{H}_2\text{O}/\text{qTS1})$                 |                                     |              |                   |                   |              |                                  |              |                   |                   |                          |                   |
| B3LYP   | 15.5                                | 25.6         | 27.2              | 26.8              | −3.2         | 12.3                             | 22.4         | 24.0              | 23.7              | 2.3                      | 29.2              |
| B971  | 17.9                                | 25.6         | 27.2              | 26.9              | −3.5         | 14.4                             | 22.1         | 23.7              | 23.4              | 2.3                      | 29.2              |
| BPW91   | 6.7                                 | 26.0         | 27.6              | 27.2              | −3.0         | 3.8                              | 23.0         | 24.7              | 24.2              | 2.5                      | 29.7              |
| M06   | 24.3                                | 25.3         | 26.9              | 26.6              | −4.0         | 20.3                             | 21.2         | 22.8              | 22.5              | 2.1                      | 28.7              |
| M06-HF  | 30.3                                | 25.9         | 27.7              | 27.8              | −3.3         | 27.0                             | 22.6         | 24.5              | 24.6              | 1.5                      | 29.3              |
| M06-L   | 10.9                                | 25.8         | 27.5              | 27.1              | −3.7         | 7.2                              | 22.1         | 23.8              | 23.4              | 2.3                      | 29.4              |
| M06-2X  | 28.7                                | 25.6         | 27.3              | 27.2              | −3.4         | 25.4                             | 22.2         | 24.0              | 23.9              | 1.8                      | 29.1              |
| MPW1K   | 22.9                                | 25.6         | 27.2              | 26.9              | −3.5         | 19.5                             | 22.2         | 23.7              | 23.4              | 2.1                      | 29.0              |
| average   | 19.7                                | 25.7         | 27.3              | 27.1              | −3.4         | 16.2                             | 22.2         | 23.9              | 23.6              | 2.1                      | 29.2              |
| MUE   | 6.9                                 | 0.2          | 0.2               | 0.3               | 0.2          | 6.8                              | 0.3          | 0.4               | 0.5               | 0.2                      | 0.2               |
| $\Delta E(\text{qFe}+\text{H}_2\text{O}/\text{qHFeOH})$               |                                     |              |                   |                   |              |                                  |              |                   |                   |                          |                   |
| CCSD  | −27.1                               | −30.9        | −29.2             | −28.4             | −2.8         | −29.9                            | −33.7        | −32.0             | −31.2             | 3.0                      | −25.4             |
| B3LYP   | −34.0                               | −30.9        | −29.2             | −28.4             | −3.0         | −37.0                            | −33.9        | −32.1             | −31.4             | 2.7                      | −25.7             |
| B971  | −33.0                               | −30.9        | −29.2             | −28.4             | −3.1         | −36.0                            | −34.0        | −32.2             | −31.5             | 2.6                      | −25.8             |
| BPW91   | −35.3                               | −30.2        | −28.5             | −27.9             | −2.7         | −38.0                            | −32.9        | −31.2             | −30.6             | 3.0                      | −24.9             |
| M06   | −26.7                               | −30.7        | −29.0             | −28.3             | −3.1         | −29.8                            | −33.9        | −32.1             | −31.4             | 2.5                      | −25.8             |
| M06-HF  | −30.7                               | −30.3        | −28.2             | −27.2             | −2.8         | −33.5                            | −33.1        | −31.0             | −30.1             | 3.1                      | −24.1             |
| M06-L   | −39.2                               | −30.8        | −29.1             | −28.3             | −3.1         | −42.3                            | −33.9        | −32.2             | −31.5             | 2.4                      | −25.9             |
| M06-2X  | −28.1                               | −30.8        | −28.9             | −28.0             | −2.9         | −30.9                            | −33.7        | −31.8             | −30.9             | 3.0                      | −25.1             |
| MPW1K   | −32.8                               | −30.9        | −29.2             | −28.4             | −3.7         | −36.5                            | −34.6        | −32.9             | −32.1             | 2.1                      | −26.3             |
| average   | −31.9                               | −30.7        | −28.9             | −28.2             | −3.0         | −34.9                            | −33.7        | −32.0             | −31.2             | 2.7                      | −25.4             |
| MUE   | 3.3                                 | 0.2          | 0.3               | 0.3               | 0.2          | 3.4                              | 0.3          | 0.4               | 0.4               | 0.3                      | 0.5               |
| $\Delta E(\text{qFe}+\text{H}_2\text{O}/\text{qTS2})$                 |                                     |              |                   |                   |              |                                  |              |                   |                   |                          |                   |
| CCSD  | 55.2                                | 39.2         | 43.0              | 41.1              | −4.7         | 50.6                             | 34.6         | 38.3              | 36.4              | 0.9                      | 42.0              |
| B3LYP   | 26.5                                | 39.1         | 42.6              | 40.7              | −4.7         | 21.8                             | 34.4         | 37.9              | 36.0              | 0.9                      | 41.6              |
| B971  | 27.6                                | 38.9         | 42.5              | 40.6              | −4.7         | 23.0                             | 34.3         | 37.9              | 35.9              | 0.9                      | 41.5              |
| BPW91   | 11.3                                | 39.1         | 42.2              | 40.6              | −4.7         | 6.6                              | 34.3         | 37.5              | 35.9              | 0.8                      | 41.5              |
| M06   | 37.6                                | 39.0         | 42.5              | 40.6              | −4.6         | 33.0                             | 34.5         | 37.9              | 36.1              | 1.0                      | 41.6              |
| M06-HF  | 58.9                                | 38.6         | 42.7              | 41.3              | −3.5         | 55.4                             | 35.2         | 39.3              | 37.9              | 1.9                      | 43.3              |
| M06-L   | 18.5                                | 39.0         | 42.3              | 40.8              | −4.9         | 13.6                             | 34.1         | 37.4              | 35.9              | 0.7                      | 41.5              |
| M06-2X  | 50.3                                | 37.0         | 41.1              | 38.7              | −4.1         | 46.1                             | 32.8         | 36.9              | 34.6              | 1.4                      | 40.1              |
| MPW1K   | 43.6                                | 38.4         | 42.5              | 40.6              | −4.3         | 39.3                             | 34.2         | 38.2              | 36.3              | 1.2                      | 41.8              |
| average   | 36.6                                | 38.7         | 42.4              | 40.6              | −4.5         | 32.2                             | 34.3         | 37.9              | 36.1              | 1.1                      | 41.6              |
| MUE   | 13.9                                | 0.5          | 0.3               | 0.4               | 0.3          | 14.1                             | 0.4          | 0.4               | 0.5               | 0.3                      | 0.5               |

Table 5. Continued

| method   | $\Delta E$ (without ZPE correction) |         |              |                   | ZPE     | $\Delta E$ (with ZPE correction) |         |              |                   | $\Delta G_{\text{corr}}$ | $\Delta G$        |
|--|-------------------------------------|---------|--------------|-------------------|---------|----------------------------------|---------|--------------|-------------------|--------------------------|-------------------|
|  |                                     |         |              |                   | corr.   |                                  |         |              |                   |                          |                   |
|  | first                               | CCSD(T) | CCSD(T)-DKH2 | CCSD(T)-3s3p-DKH2 | first   | first                            | CCSD(T) | CCSD(T)-DKH2 | CCSD(T)-3s3p-DKH2 | first                    | CCSD(T)-3s3p-DKH2 |
| basis set on   | column                              |         |              |                   | column  | column                           |         |              |                   | column                   |                   |
| Fe   | cc-pVTZ                             | cc-pVnZ | cc-pVnZ-DK   | cc-pwCVnZ-DK      | cc-pVTZ | cc-pVTZ                          | cc-pVnZ | cc-pVnZ-DK   | cc-pwCVnZ-DK      | cc-pVTZ                  | cc-pwCVnZ-DK      |
| $\Delta E(\text{qFe}+\text{H}_2\text{O}/\text{qH}_2\text{FeO})$  |                                     |         |              |                   |         |                                  |         |              |                   |                          |                   |
| CCSD   | 36.6                                | 22.0    | 24.3         | 22.9              | −3.2    | 33.4                             | 18.8    | 21.1         | 19.7              | 2.6                      | 25.4              |
| B3LYP  | 10.6                                | 21.8    | 24.1         | 22.6              | −3.8    | 6.8                              | 18.0    | 20.3         | 18.8              | 2.2                      | 24.8              |
| B971   | 14.8                                | 21.8    | 24.0         | 22.5              | −3.9    | 10.9                             | 17.9    | 20.1         | 18.6              | 2.0                      | 24.6              |
| BPW91  | −9.7                                | 25.8    | 27.4         | 25.4              | −3.4    | −13.1                            | 22.4    | 24.0         | 22.0              | 2.1                      | 27.6              |
| M06  | 24.1                                | 21.8    | 24.0         | 22.4              | −4.1    | 20.0                             | 17.8    | 19.9         | 18.3              | 1.8                      | 24.2              |
| M06-HF   | 54.0                                | 24.9    | 27.2         | 25.9              | −3.6    | 50.4                             | 21.2    | 23.5         | 22.3              | 1.3                      | 27.2              |
| M06-L  | −0.5                                | 26.2    | 27.7         | 25.8              | −3.4    | −4.0                             | 22.8    | 24.2         | 22.3              | 2.1                      | 27.9              |
| M06-2X   | 41.6                                | 23.6    | 26.0         | 24.7              | −3.9    | 37.7                             | 19.7    | 22.1         | 20.8              | 0.8                      | 25.5              |
| MPW1K  | −76.5                               | 22.2    | 24.5         | 23.1              | −4.5    | −81.1                            | 17.7    | 20.0         | 18.6              | 1.5                      | 24.6              |
| average  | 10.5                                | 23.3    | 25.5         | 23.9              | −3.8    | 6.8                              | 19.6    | 21.7         | 20.2              | 1.8                      | 25.8              |
| MUE  | 26.3                                | 1.6     | 1.4          | 1.4               | 0.3     | 26.3                             | 1.7     | 1.6          | 1.5               | 0.4                      | 1.2               |
| $\Delta E(\text{qFe}+\text{H}_2\text{O}/\text{qFeO}+\text{H}_2)$ |                                     |         |              |                   |         |                                  |         |              |                   |                          |                   |
| CCSD   | 41.7                                | 32.5    | 34.3         | 33.3              | −6.1    | 35.5                             | 26.3    | 28.1         | 27.2              | −6.1                     | 27.2              |
| B3LYP  | 16.6                                | 32.4    | 34.2         | 33.1              | −5.7    | 10.8                             | 26.6    | 28.4         | 27.4              | −5.6                     | 27.5              |
| B971   | 22.0                                | 32.4    | 34.2         | 33.2              | −5.8    | 16.2                             | 26.6    | 28.4         | 27.4              | −5.7                     | 27.4              |
| BPW91  | −1.4                                | 32.3    | 34.0         | 32.9              | −5.5    | −6.9                             | 26.7    | 28.5         | 27.4              | −5.4                     | 27.5              |
| M06  | 33.6                                | 32.4    | 34.2         | 33.2              | −6.1    | 27.5                             | 26.3    | 28.1         | 27.1              | −6.0                     | 27.2              |
| M06-HF   | 61.1                                | 42.4    | 36.3         | 35.7              | −5.8    | 55.2                             | 36.5    | 30.5         | 29.8              | −5.8                     | 29.8              |
| M06-L  | 12.8                                | 32.4    | 34.2         | 33.2              | −4.9    | 7.9                              | 27.5    | 29.3         | 28.3              | −5.9                     | 27.3              |
| M06-2X   | 48.9                                | 41.0    | 40.4         | 40.2              | −6.0    | 42.9                             | 35.0    | 34.4         | 34.2              | −5.9                     | 34.2              |
| MPW1K  | 38.7                                | 32.4    | 34.2         | 33.2              | −6.0    | 32.7                             | 26.4    | 28.2         | 27.2              | −5.9                     | 27.3              |
| average  | 30.4                                | 34.4    | 35.1         | 34.2              | −5.8    | 24.7                             | 28.7    | 29.3         | 28.4              | −5.8                     | 28.4              |
| MUE  | 15.9                                | 3.2     | 1.5          | 1.6               | 0.3     | 15.7                             | 3.1     | 1.4          | 1.6               | 0.2                      | 1.6               |

<sup>a</sup> Calculations presented in this table were performed using unrestricted methods; methods used for geometry optimization and frequency calculations are specified in the first column (the results of these calculations are shown in columns 2, 6, 7, and 11). Additional single-point energies were obtained using the CBS2 scheme with bases of triple- $\zeta$  and quadruple- $\zeta$  cardinality (i.e.,  $n = 3$  and 4).

with (augmented) and without diffuse functions (aug-cc-pVnZ vs cc-pVnZ) for all methods listed in Table 4. The average differences between the CBS2 energies calculated with the two basis sets were 0.4 and 0.3 kcal/mol for qFe+H<sub>2</sub>O/qTS1 and qFe+H<sub>2</sub>O/qHFeOH, respectively. For the post-HF methods the differences were less than 0.2 kcal/mol. This shows that reasonable accuracy with respect to the CBS limit and computational demands can be using basis sets without diffusion functions. It is worth noting that double- $\zeta$  basis sets do not provide sufficiently accurate results (Figure 2), and so the CBS limit should be calculated from TZ and QZ basis sets at least.

The final goal of our study was to explore the potential energy surfaces of the reaction between Fe and H<sub>2</sub>O as accurately as possible. In light of the results reported in the preceding paragraphs and sections III.A and III.B, we adopted the following scheme: (1) geometry optimization was performed using all of the considered DFT methods with the cc-pVTZ basis set, (2) frequencies and zero-point energy corrections using the harmonic approximation were obtained at the same levels of theory, (3) single-point uCCSD(T) energy calculations using CBS extrapolation from the cc-pVTZ and cc-pVQZ basis sets were carried

out, or, alternatively, (4) the scalar relativistic uCCSD(T)-DKH2 and valence plus outer-core (3s3p3d4s) electronic correlation CCSD(T)-3s3p-DKH2 calculations were also performed using the CBS limit and the cc-pVnZ-DK or cc-pwCVnZ-DK basis sets, respectively. In order to verify that the ground electronic state of the Fe + H<sub>2</sub>O reaction coordinate retained the quintet multiplicity<sup>47–49,51</sup> and that no crossing occurred, we also performed calculations for different multiplicities. Figure 3 shows the lowest energies for the quintet state and that there is no crossing between the quintet and triplet surfaces. The only limitation of our approach is the single-reference description; some stationary points on the PES (specifically, the TS) may have some multireference character. Bias in the energies attributable to this can be measured using the T<sub>1</sub> diagnostic for coupled cluster methods. Problems due to spin contamination can also be partially relieved by using coupled cluster methods, which are quite effective at reducing uHF spin contamination to acceptable levels.<sup>53</sup> In this context, the results obtained for Fe and FeO with coupled cluster methods (including  $\langle S^2 \rangle$  and T<sub>1</sub> values) are discussed in sections III.A and III.B, respectively. For a single-point energy calculation at the uCCSD(T)-3s3p-DKH2 level on



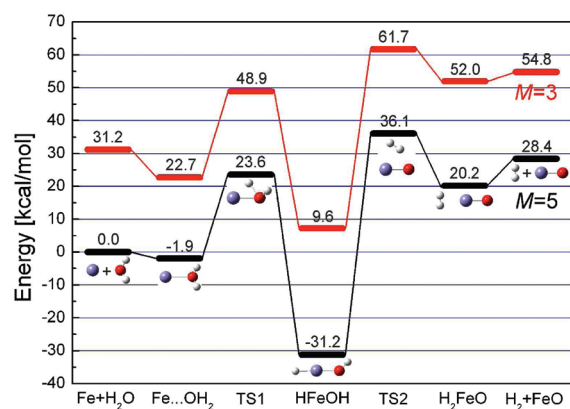


**Figure 3.** Reaction scheme showing the stationary points on the quintet (multiplicity  $M = 5$ ) and triplet ( $M = 3$ ) PES along the path of the  $\text{Fe} + \text{H}_2\text{O}$  reaction in the gas phase, with ZPVE corrections. The reported energies are the averages of the CCSD(T)-3s3p-DKH2/CBS2 values reported in the 10th column of Table 5 for  $M = 5$ .

the transition state qTS1, we obtained  $\langle S^2 \rangle \approx 6.7$  (vs expected  $S(S + 1) = 6$ ) for the uHF wave function; however, the  $T_1$  diagnostic had an acceptable value (below 0.03). The single-reference description is fully adequate for the global minimum (qHFeOH), for which  $\langle S^2 \rangle \approx 6.03$  and  $T_1 < 0.022$ . The only potentially problematic stationary point could be transition state TS2; for the uHF wave function for this species,  $\langle S^2 \rangle \approx 6.9$  and  $T_1 < 0.12$ . The value of the  $T_1$  diagnostic indicates that this transition state has some multireference character. However, the accuracy of energy corresponding to this transition state is not crucial for practical purposes and the final goal of this study, to explore the kinetics and the thermodynamics of the reaction between Fe and  $\text{H}_2\text{O}$ . In terms of the performance of the different methods used, the trends shown in Table 5 for the  $\text{Fe} + \text{H}_2\text{O}$  reaction mirror those observed in Tables 3 and 4, which report the thermochemical data for FeO and  $\text{Fe}(\text{OH})_2$ ; the different density functionals all afford very different energies, but all of the single-point CCSD(T) energies obtained at the different DFT geometries are very similar. This again suggests that the regions surrounding the stationary points on the PES of the  $\text{Fe} + \text{H}_2\text{O}$  reaction are quite flat.

The results obtained by examining all the stationary points on the  $\text{Fe} + \text{H}_2\text{O}$  potential energy surface using the method described above are collected in Table 5 and visualized in Figure 3 (the energies reported in this figure are an average of the CCSD(T)-3s3p-DKH2/CBS2 energies from the 10th column of Table 5 for  $M = 5$ ; for  $M = 3$  only three values for such average were used). In the computed reaction mechanism, the iron atom forms a noncovalent complex with the water molecule. The two react via transition state qTS1 ( $\text{Fe}(4s^{1.1}3d^{6.3}4p^{0.1})\text{H}(1s^{0.9})\text{O}(2s^{1.8}2p^{5.2})\text{H}(1s^{0.5})$ ) to form the highly stable qHFeOH intermediate ( $\text{H}(1s^{1.5})\text{Fe}(4s^{0.5}3d^{6.2}4p^{0.2})\text{O}(2s^{1.8}2p^{5.3})\text{H}(1s^{0.5})$ ), which is expected to be the dominant reaction intermediate. We also identified a local minimum labeled qH<sub>2</sub>FeO that was not mentioned in ref 48 but is discussed in refs 49 and 51. The overall mechanism of the  $\text{Fe} + \text{H}_2\text{O}$  reaction is in qualitative agreement with that reported in previous publications.<sup>48,49,51</sup> However, in quantitative terms, there are various inconsistencies in the literature data on this reaction. A wide range of values (all of which include the ZPE correction) have been reported for the energy barrier that is most important in understanding the reaction's kinetics,  $\text{qFe} + \text{H}_2\text{O}/\text{qTS1}$ . Specifically,

this barrier has been calculated to be 14.8<sup>48</sup> (B3LYP/6-311+G-(3df,2p)), 32.7<sup>48</sup> (CCSD(T)/6-311G\*\*), 8.6<sup>49</sup> (B3LYP/6-311++G(d,p)), and 14.3 kcal/mol<sup>51</sup> (B3LYP/6-311+G(2d,p)) compared with our benchmark value (including ZPE correction) of 23.6 kcal/mol (the average of the CCSD(T)-3s3p-DKH2/CBS2 values in the 10th column of Table 5). The large deviations can be attributed to the small basis sets and DFT methods used in the previous literature studies (cf. Figure 2 and Table 4). Similarly, literature values for the energy difference between the reactants and the global minimum on the PES ( $\text{qFe} + \text{H}_2\text{O}/\text{qHFeOH}$ ) are very different, although the deviation between the literature data and our benchmark is less pronounced in this case: previous results include -34.2<sup>48</sup> (B3LYP/6-311+G(3df,2p)), -26.2<sup>48</sup> (CCSD(T)/6-311G\*\*), -41.1<sup>49</sup> (B3LYP/6-311++G(d,p)), and -35.6 kcal/mol<sup>51</sup> (B3LYP/6-311+G(2d,p)) compared with our value of -31.2 kcal/mol (CCSD(T)-3s3p-DKH2/CBS2).

## IV. CONCLUSIONS

The quantum chemical study reported herein examined the simplest model system for studying the reaction of nZVI with water, i.e., the gas-phase reaction of an iron atom with a water molecule. This simple model was used to compare the performance of various widely used DFT functionals to that of highly accurate post-HF methods and multireference quantum chemical methods that can properly account for electron correlation and scalar relativistic effects. The calculations illustrate the following. (i) Inclusion of dynamic electron correlation is essential for a proper description of this reaction. (ii) The PES around the stationary points along the reaction path is rather flat; various methods that account for dynamic electron correlation can be used for geometry optimizations, and scalar relativistic effects do not significantly affect the calculated geometries. (iii) The only single-point energies that were in reasonable agreement with the experimental data were those calculated at the CCSD(T)/CBS level; the DFT and post-HF single reference methods gave inaccurate results. (iv) Direct interpretation of DFT energies can be unproductive in the absence of either benchmark data obtained at the recommended level of theory or experimental data, (v) Scalar relativistic effects are small in this system, but their magnitude is still in the same sort of range as chemical accuracy ( $\pm 1$  kcal/mol). (vi) The multireference character of intermediates and potential spin contamination should always be carefully examined. The CCSD(T)-3s3p-DKH2/CBS2 method can be considered a gold standard for the reaction in question because results obtained at this level are in good agreement with experimental atomic excitation energies and thermochemical data. The gas-phase activation energy (including the ZPVE correction) of the  $\text{Fe} + \text{H}_2\text{O}$  reaction is 23.6 kcal/mol ( $\Delta G_{298\text{K}}^{\ddagger} = 29.2$  kcal/mol); HFeOH is a stable intermediate lying -31.2 kcal/mol below reactants ( $\Delta G_{298\text{K}} = -25.4$  kcal/mol).

## ■ AUTHOR INFORMATION

### Corresponding Author

\*E-mail: frantisek.karlicky@upol.cz (F.K.), michal.otyepka@upol.cz (M.O.).

## ■ ACKNOWLEDGMENT

Financial support from the Czech Science Foundation (GACR P208/11/P463), the Operational Program Research



and Development for Innovations-European Regional Development Fund (CZ.1.05/2.1.00/03.0058), and the Operational Program Education for Competitiveness-European Social Fund (CZ.1.07/2.3.00/20.0017) is gratefully acknowledged. We thank Dana Nachtigalova (IOCHB, Prague) for critical comments and helpful discussions.

## REFERENCES

- Tratnyek, P. G.; Johnson, R. L. *Nano Today* **2006**, *1*, 44–48.
- Zhang, W. X. *J. Nanopart. Res.* **2003**, *5*, 323–332.
- Li, X. Q.; Elliott, D. W.; Zhang, W. X. *Crit. Rev. Solid State* **2006**, *31*, 111–122.
- Cundy, A. B.; Hopkinson, L.; Whitby, R. L. D. *Sci. Total Environ.* **2008**, *400*, 42–51.
- Amonette, J. E.; Sarathy, V.; Linehan, J. C.; Matson, D. W.; Wang, C.; Nurmi, J. T.; Pecher, K.; Penn, R. L.; Tratnyek, P. G.; Baer, D. R. *Geochim. Cosmochim. Acta* **2005**, *69*, A263–A263.
- Arnold, W. A.; Roberts, A. L. *Environ. Sci. Technol.* **2000**, *34*, 1794–1805.
- Bandstra, J. Z.; Miehr, R.; Johnson, R. L.; Tratnyek, P. G. *Environ. Sci. Technol.* **2005**, *39*, 230–238.
- Gillham, R. W.; Ohannesin, S. F. *Ground Water* **1994**, *32*, 958–967.
- Johnson, T. L.; Fish, W.; Gorby, Y. A.; Tratnyek, P. G. *J. Contam. Hydrol.* **1998**, *29*, 379–398.
- Kim, J. H.; Tratnyek, P. G.; Chang, Y. S. *Environ. Sci. Technol.* **2008**, *42*, 4106–4112.
- Nam, S.; Tratnyek, P. G. *Water Res.* **2000**, *34*, 1837–1845.
- Roberts, A. L.; Totten, L. A.; Arnold, W. A.; Burris, D. R.; Campbell, T. J. *Environ. Sci. Technol.* **1996**, *30*, 2654–2659.
- Sarathy, V.; Salter, A. J.; Nurmi, J. T.; Johnson, G. O.; Johnson, R. L.; Tratnyek, P. G. *Environ. Sci. Technol.* **2010**, *44*, 787–793.
- Sayles, G. D.; You, G. R.; Wang, M. X.; Kupferle, M. J. *Environ. Sci. Technol.* **1997**, *31*, 3448–3454.
- Wang, C. B.; Zhang, W. X. *Environ. Sci. Technol.* **1997**, *31*, 2154–2156.
- Alowitz, M. J.; Scherer, M. M. *Environ. Sci. Technol.* **2002**, *36*, 299–306.
- Darab, J. G.; Amonette, A. B.; Burke, D. S. D.; Orr, R. D.; Ponder, S. M.; Schrick, B.; Mallouk, T. E.; Lukens, W. W.; Caulder, D. L.; Shuh, D. K. *Chem. Mater.* **2007**, *19*, 5703–5713.
- Miehr, R.; Tratnyek, P. G.; Bandstra, J. Z.; Scherer, M. M.; Alowitz, M. J.; Bylaska, E. J. *Environ. Sci. Technol.* **2004**, *38*, 139–147.
- Ponder, S. M.; Darab, J. G.; Bucher, J.; Caulder, D.; Craig, I.; Davis, L.; Edelstein, N.; Lukens, W.; Nitsche, H.; Rao, L. F.; Shuh, D. K.; Mallouk, T. E. *Chem. Mater.* **2001**, *13*, 479–486.
- Ponder, S. M.; Darab, J. G.; Mallouk, T. E. *Environ. Sci. Technol.* **2000**, *34*, 2564–2569.
- Ponder, S. M.; Ford, J. R.; Darab, J. G.; Mallouk, T. E.; Ferragels: A new family of materials for remediation of aqueous metal ion solutions. In *Scientific Basis for Nuclear Waste Management XXII*; Wronkiewicz, D. J., Lee, J. H., Eds.; Materials Research Society: Warrendale, PA, 1999; Vol. 556, pp 1269–1276.
- Su, C. M.; Puls, R. W. *Environ. Sci. Technol.* **2001**, *35*, 4562–4568.
- Su, C. M.; Puls, R. W. *Environ. Sci. Technol.* **2001**, *35*, 1487–1492.
- Lanzani, G.; Nasibulin, A. G.; Laasonen, K.; Kauppinen, E. I. *Nano Res.* **2009**, *2*, 660–670.
- Lanzani, G.; Nasibulin, A. G.; Laasonen, K.; Kauppinen, E. I. *J. Phys. Chem. C* **2009**, *113*, 12939–12942.
- Lim, D. H.; Lastoskie, C. M. *Environ. Sci. Technol.* **2009**, *43*, 5443–5448.
- Lim, D. H.; Lastoskie, C. M.; Soon, A.; Becker, U. *Environ. Sci. Technol.* **2009**, *43*, 1192–1198.
- DeYonker, N. J.; Peterson, K. A.; Steyl, G.; Wilson, A. K.; Cundari, T. R. *J. Phys. Chem. A* **2007**, *111*, 11269–11277.
- Schultz, N. E.; Zhao, Y.; Truhlar, D. G. *J. Phys. Chem. A* **2005**, *109*, 11127–11143.
- Yang, Y.; Weaver, M. N.; Merz, K. M. *J. Phys. Chem. A* **2009**, *113*, 9843–9851.
- Li, S. G.; Hennigan, J. M.; Dixon, D. A.; Peterson, K. A. *J. Phys. Chem. A* **2009**, *113*, 7861–7877.
- Tekarli, S. M.; Drummond, M. L.; Williams, T. G.; Cundari, T. R.; Wilson, A. K. *J. Phys. Chem. A* **2009**, *113*, 8607–8614.
- Hubner, O.; Sauer, J. *J. Chem. Phys.* **2002**, *116*, 617–628.
- Hubner, O.; Sauer, J. *Collect. Czech. Chem. Commun.* **2003**, *68*, 405–422.
- Roithová, J.; Schröder, D. *Chem. Rev.* **2010**, *110*, 1170–1211.
- Schröder, D. *J. Phys. Chem. A* **2008**, *112*, 13215–13224.
- Knowles, P. J.; Werner, H. J. *Chem. Phys. Lett.* **1985**, *115*, 259–267.
- Zilberberg, I.; Gora, R. W.; Zhidomirov, G. M.; Leszczynski, J. *J. Chem. Phys.* **2002**, *117*, 7153–7161.
- Balabanov, N. B.; Peterson, K. A. *J. Chem. Phys.* **2006**, *125*, 074110.
- Cundari, T. R.; Leza, H. A. R.; Grimes, T.; Steyl, G.; Waters, A.; Wilson, A. K. *Chem. Phys. Lett.* **2005**, *401*, 58–61.
- Ilias, M.; Kello, V.; Urban, M. *Acta Phys. Slovaca* **2010**, *60*, 259–391.
- Martin, J.; Baker, J.; Pulay, P. *J. Comput. Chem.* **2009**, *30*, 881–883.
- Bally, T.; Borden, W. T. Calculations on Open-Shell molecules: A Beginner's Guide. In *Reviews in Computational Chemistry*; Lipkowitz, K. B., Boyd, D. B., Eds.; Wiley: New York, 1999; Vol. 13, pp 1–97.
- Matxain, J. M.; Mercero, J. M.; Irigoras, A.; Ugalde, J. M. *Mol. Phys.* **2004**, *102*, 2635–2637.
- Camaioni, D. M.; Ginovska, B.; Dupuis, M. *J. Phys. Chem. C* **2009**, *113*, 1830–1836.
- Parkinson, G. S.; Dohnalek, Z.; Smith, R. S.; Kay, B. D. *J. Phys. Chem. C* **2009**, *113*, 1818–1829.
- Rollason, R. J.; Plane, J. M. C. *Phys. Chem. Chem. Phys.* **2000**, *2*, 2335–2343.
- Mebel, A. M.; Hwang, D. Y. *J. Phys. Chem. A* **2001**, *105*, 7460–7467.
- Zhang, L. N.; Zhou, M. F.; Shao, L. M.; Wang, W. N.; Fan, K. N.; Qin, Q. Z. *J. Phys. Chem. A* **2001**, *105*, 6998–7003.
- Gutsev, G. L.; Mochena, M. D.; Bauschlicher, C. W. *Chem. Phys.* **2005**, *314*, 291–298.
- Self, D. E.; Plane, J. M. C. *Phys. Chem. Chem. Phys.* **2003**, *5*, 1407–1418.
- Balabanov, N. B.; Peterson, K. A. *J. Chem. Phys.* **2005**, *123*, 064107.
- Stanton, J. F. *J. Chem. Phys.* **1994**, *101*, 371–374.
- Lee, T. J. *Chem. Phys. Lett.* **2003**, *372*, 362–367.
- Lee, T. J.; Taylor, P. R. *Int. J. Quantum Chem.* **1989**, 199–207.
- Janssen, C. L.; Nielsen, I. M. B. *Chem. Phys. Lett.* **1998**, *290*, 423–430.
- Becke, A. D. *J. Chem. Phys.* **1993**, *98*, 5648–5652.
- Becke, A. D. *Phys. Rev. A* **1988**, *38*, 3098–3100.
- Perdew, J. P.; Wang, Y. *Phys. Rev. B* **1992**, *45*, 13244–13249.
- Gutsev, G. L.; Mochena, M. D.; Johnson, E.; Bauschlicher, C. W. *J. Chem. Phys.* **2006**, *125*, 194312.
- Gutsev, G. L.; Bauschlicher, C. W. *Chem. Phys.* **2003**, *291*, 27–40.
- Gutsev, G. L.; Khanna, S. N.; Rao, B. K.; Jena, P. *J. Phys. Chem. A* **1999**, *103*, 5812–5822.
- Vitek, A.; Kalus, R.; Paidarova, I. *Phys. Chem. Chem. Phys.* **2010**, *12*, 13657–13666.
- Sousa, S. F.; Fernandes, P. A.; Ramos, M. J. *J. Phys. Chem. A* **2007**, *111*, 10439.
- Zhao, Y.; Truhlar, D. G. *Theor. Chem. Acc.* **2008**, *120*, 215–241.
- Zhao, Y.; Truhlar, D. G. *J. Chem. Phys.* **2006**, *125*, 194101.

- (67) Lynch, B. J.; Fast, P. L.; Harris, M.; Truhlar, D. G. *J. Phys. Chem. A* **2000**, *104*, 4811–4815.
- (68) Schuchardt, K. L.; Didier, B. T.; Elsethagen, T.; Sun, L. S.; Gurumoorathi, V.; Chase, J.; Li, J.; Windus, T. L. *J. Chem. Inf. Model* **2007**, *47*, 1045–1052.
- (69) Halkier, A.; Helgaker, T.; Jorgensen, P.; Klopper, W.; Olsen, J. *Chem. Phys. Lett.* **1999**, *302*, 437–446.
- (70) Williams, T. G.; DeYonker, N. J.; Wilson, A. K. *J. Chem. Phys.* **2008**, *128*, 044101.
- (71) Halkier, A.; Helgaker, T.; Jorgensen, P.; Klopper, W.; Koch, H.; Olsen, J.; Wilson, A. K. *Chem. Phys. Lett.* **1998**, *286*, 243–252.
- (72) Frisch, M. J.; Trucks, G. W.; Schlegel, H. B.; Scuseria, G. E.; Robb, M. A.; Cheeseman, J. R.; Scalmani, G.; Barone, V.; Mennucci, B.; Petersson, G. A.; Nakatsuji, H.; Caricato, M.; Li, X.; Hratchian, H. P.; Izmaylov, A. F.; Bloino, J.; Zheng, G.; Sonnenberg, J. L.; Hada, M.; Ehara, M.; Toyota, K.; Fukuda, R.; Hasegawa, J.; Ishida, M.; Nakajima, T.; Honda, Y.; Kitao, O.; Nakai, H.; Vreven, T.; J. A. Montgomery, J.; Peralta, J. E.; Ogliaro, F.; Bearpark, M.; Heyd, J. J.; Brothers, E.; Kudin, K. N.; Staroverov, V. N.; Kobayashi, R.; Normand, J.; Raghavachari, K.; Rendell, A.; Burant, J. C.; Iyengar, S. S.; Tomasi, J.; Cossi, M.; Rega, N.; Millam, J. M.; Klene, M.; Knox, J. E.; Cross, J. B.; Bakken, V.; Adamo, C.; Jaramillo, J.; Gomperts, R.; Stratmann, R. E.; Yazyev, O.; Austin, A. J.; Cammi, R.; Pomelli, C.; Ochterski, J. W.; Martin, R. L.; Morokuma, K.; Zakrzewski, V. G.; Voth, G. A.; Salvador, P.; Dannenberg, J. J.; Dapprich, S.; Daniels, A. D.; Farkas, Ö.; Foresman, J. B.; Ortiz, J. V.; Cioslowski, J.; Fox, D. J. *Gaussian 09*, Revision A.02; Gaussian, Inc.: Wallingford, CT, 2009.
- (73) Werner, H.-J.; Knowles, P. J.; Lindh, R.; Manby, F. R.; Schütz, M.; Celani, P.; Korona, T.; Mitrushenkov, A.; Rauhut, G.; Adler, T. B.; Amos, R. D.; Bernhardsson, A.; Berning, A.; Cooper, D. L.; Deegan, M. J. O.; Dobbyn, A. J.; Eckert, F.; Goll, E.; Hampel, C.; Hetzer, G.; Hrenar, T.; Knizia, G.; Köppl, C.; Liu, Y.; Lloyd, A. W.; Mata, R. A.; May, A. J.; McNicholas, S. J.; Meyer, W.; Mura, M. E.; Nicklass, A.; Palmieri, P.; Pflüger, K.; Pitzer, R.; Reiher, M.; Schumann, U.; Stoll, H.; Stone, A. J.; Tarroni, R.; Thorsteinsson, T.; Wang, M.; Wolf, A. *MOLPRO*, version 2006.1, a package of *ab initio* programs; University College Cardiff Consultants Limited: Cardiff, UK, 2006; <http://www.molpro.net>.
- (74) Saunders, V. R.; Hillier, I. H. *Int. J. Quantum Chem.* **1973**, *7*, 699–705.
- (75) Rabuck, A. D.; Scuseria, G. E. *J. Chem. Phys.* **1999**, *110*, 695–700.
- (76) Sansonetti, J. E.; Martin, W. C.; Young, S. L. *Handbook of Basic Atomic Spectroscopic Data* (version 1.1.2); National Institute of Standards and Technology: Gaithersburg, MD, 2005; <http://physics.nist.gov/Handbook>.
- (77) Chase, M. W. *NIST-JANAF Thermochemical Tables*, 4th ed. (*J. Phys. Chem. Ref. Data, Monograph No. 9*); American Chemical Society and American Institute of Physics: Woodbury, NY, 1988.
- (78) Cheung, A. S. C.; Gordon, R. M.; Merer, A. J. *J. Mol. Spectrosc.* **1981**, *87*, 289–296.
- (79) Cheung, A. S. C.; Lee, N.; Lyyra, A. M.; Merer, A. J.; Taylor, A. W. *J. Mol. Spectrosc.* **1982**, *95*, 213–225.
- (80) Jensen, D. E.; Jones, G. A. *J. Chem. Soc., Faraday Trans. 1* **1973**, *69*, 1448–1454.
- (81) Murad, E. *J. Chem. Phys.* **1980**, *73*, 1381–1385.
- (82) Sakellaris, C. N.; Miliordos, E.; Mavridis, A. *J. Chem. Phys.* **2011**, *134*, 234308.
- (83) Kellogg, C. B.; Irikura, K. K. *J. Phys. Chem. A* **1999**, *103*, 1150–1159.
- (84) Drechsler, G.; Boesl, U.; Bassmann, C.; Schlag, E. W. *J. Chem. Phys.* **1997**, *107*, 2284–2291.